

# SynCAM 1 participates in axo-dendritic contact assembly and shapes neuronal growth cones

Massimiliano Stagi, Adam I. Fogel, and Thomas Biederer<sup>1</sup>

Department of Molecular Biophysics and Biochemistry, Yale University, New Haven, CT 06520

Edited\* by Pietro De Camilli, Yale University and Howard Hughes Medical Institute, New Haven, CT, and approved March 9, 2010 (received for review October 13, 2009)

**Neuronal growth cones are highly motile structures that tip developing neurites and explore their surroundings before axo-dendritic contact and synaptogenesis. However, the membrane proteins organizing these processes remain insufficiently understood. Here we identify that the synaptic cell adhesion molecule 1 (SynCAM 1), an immunoglobulin superfamily member, is already expressed in developing neurons and localizes to their growth cones. Upon interaction of growth cones with target neurites, SynCAM 1 rapidly assembles at these contacts to form stable adhesive clusters. Synaptic markers can also be detected at these sites. Addressing the functions of SynCAM 1 in growth cones preceding contact, we determine that it is required and sufficient to restrict the number of active filopodia. Further, SynCAM 1 negatively regulates the morphological complexity of migrating growth cones. Focal adhesion kinase, a binding partner of SynCAM 1, is implicated in its morphogenetic activities. These results reveal that SynCAM 1 acts in developing neurons to shape migrating growth cones and contributes to the adhesive differentiation of their axo-dendritic contacts.**

CADM | focal adhesion kinase | growth cone | synaptic adhesion | synaptogenesis

**G**rowth cones tip differentiating neurites and target exploration occurs through filopodia (1–3). Upon contact, axonal growth cones undergo a rapid morphological transition that initiates synaptic membrane differentiation in conjunction with the appearance of synaptic vesicles, electron-dense cleft material, and postsynaptic specializations (4–6). Although the cytoskeletal framework of growth cones is being defined (7, 8), the best understood roles of surface proteins are in outgrowth and guidance (9, 10). The roles of membrane proteins in shaping growth cones and target exploration remain less well defined.

In contrast, insight has been gained into the roles of surface proteins in synaptic differentiation. Trans-synaptic interactions of synaptic cell adhesion molecules (SynCAMs), neuroligins/neurexins, ephrinB/EphB receptors, and select other proteins organize developing synapses (11, 12). Additional proteins act in synapse maturation, notably N-cadherin (13). Although conceptually intriguing, no evidence points to roles of these proteins in axo-dendritic contact differentiation.

SynCAM 1, alternatively named CADM1/IGSF4/nectin-like 2 (14, 15), is an Ig adhesion molecule that drives synapse formation in developing neurons. SynCAM 1 is already expressed in the late embryonic and early postnatal brain, whereas the other SynCAM family members as well as neuroligins and neuroligins peak subsequently during synaptogenesis (16–19). This profile of SynCAM 1 indicates functions preceding synapse formation. We now reveal SynCAM 1 as a surface protein of axonal growth cones that assembles rapidly and stably at axo-dendritic contacts. Sites marked by SynCAM 1 can also contain synaptic markers, indicating that they have the potential to differentiate into nascent synapses. Before contact, SynCAM 1 regulates the complexity of growth cones and controls their active filopodia number, and we identify focal adhesion kinase (FAK) as a binding partner and effector in shaping growth cones. These results

demonstrate that SynCAM 1 is an early player in axo-dendritic contact differentiation and organizes growth cones through a FAK-dependent pathway.

## Results

**Growth Cones Express SynCAM 1.** To elucidate the early developmental roles of SynCAM 1, we analyzed its expression in dissociated hippocampal neurons at 5 days in vitro (d.i.v.). At this time, axons are specified and dendrites have begun to grow, but most synapses have yet to form (20). SynCAM 1 is already prominently expressed at this stage, preceding other synaptic adhesion molecules (Fig. 1*A*), and is enriched in growth cones of neurites positive for the axonal marker tau (Fig. 1*B* and Fig. S1*B*). SynCAM 1 knockout controls confirm antibody specificity (21) (Fig. 1*C* and Fig. S1*A* and *C*). These results agree with the presence of SynCAM 1 in growth cone preparations (Fig. S2) and with the recent proteomic identification of SynCAM 1 as a strongly enriched growth cone protein (22).

We next visualized SynCAM 1 in live growth cones by inserting the pH-sensitive GFP variant pHluorin (23) into the extracellular domain (see Fig. 3*B* for a model). This construct is functional as it rescues SynCAM 1 knockout phenotypes in immature neurons and is properly localized to mature synapses (see below). Live imaging of migrating growth cones identifies SynCAM 1–pHluorin in their central region and filopodia (Fig. S3), similar to endogenous SynCAM 1. To analyze the surface expression of SynCAM 1–pHluorin, we imaged growth cones while transiently lowering the extracellular pH to quench its surface-exposed pool. This leaves intracellular pHluorin molecules unaffected (Fig. S4*A* and *B*). SynCAM 1–pHluorin fluorescence in growth cones and their filopodia are almost lost at low extracellular pH, demonstrating that SynCAM 1 is expressed on the growth cone surface (Fig. S4*C–E*). We next addressed what fraction of SynCAM 1 is surface-exposed by imaging growth cones first live at neutral and then at low pH, followed by fixation, permeabilization and repeat imaging at neutral pH (Fig. 1*D*). SynCAM 1–pHluorin fluorescence was indistinguishable at both neutral pH conditions (Fig. 1*E*), demonstrating that only a small fraction resides intracellularly.

**Rapid Assembly of SynCAM 1 upon Axo-Dendritic Contact.** Filopodia participate in the rapid formation of presynaptic specializations as axonal growth cones pass dendrites (1, 24, 25). Considering the roles of SynCAM 1 in cell adhesion, we asked whether it participates in these axo-dendritic interactions of growth cones. By selecting growth cones expressing SynCAM 1–pHluorin in approach to SynCAM 1–pHluorin–marked neurites, we find that axo-

Author contributions: M.S., A.I.F., and T.B. designed research; M.S., A.I.F., and T.B. performed research; M.S., A.I.F., and T.B. analyzed data; and T.B. wrote the paper.

The authors declare no conflict of interest.

\*This Direct Submission article had a prearranged editor.

<sup>1</sup>To whom correspondence should be addressed. E-mail: thomas.biederer@yale.edu.

This article contains supporting information online at [www.pnas.org/cgi/content/full/0911798107/DCSupplemental](http://www.pnas.org/cgi/content/full/0911798107/DCSupplemental).

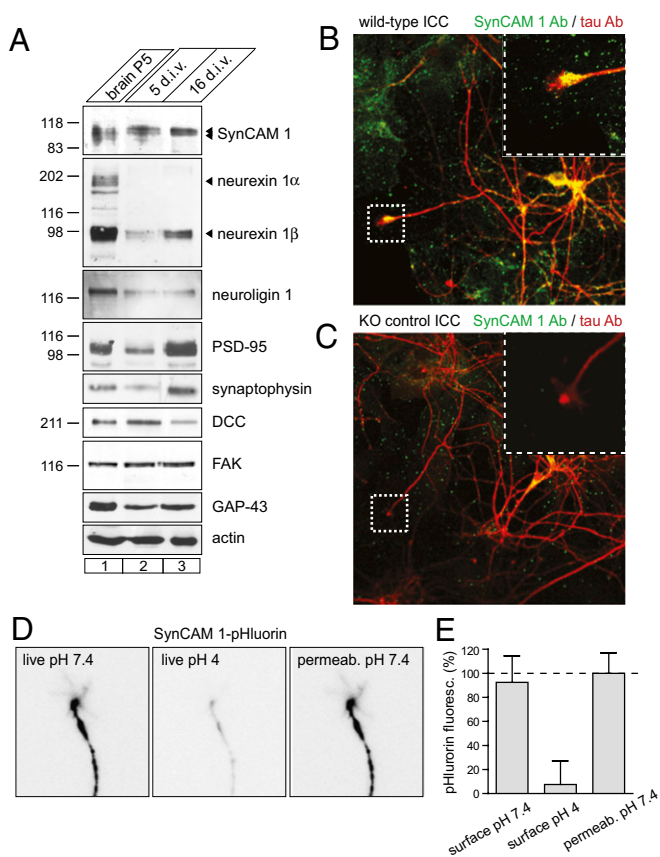


**Fig. 1.** SynCAM 1 localizes to growth cones. (A) Immunoblot analysis of neuronal culture lysates at the indicated days in vitro (d.i.v.). SynCAM 1 expression precedes the synaptic adhesion molecules neuroligin and neuroligin. PSD-95 and synaptophysin are synaptic protein controls, whereas DCC, FAK, and GAP-43 are already expressed in growth cones. Actin served as loading control, and rat forebrain from postnatal day 5 (P5) as positive control. (B and C) Confocal fluorescence image of dissociated mouse wild-type (B) and SynCAM 1 knockout (KO; C) hippocampal neurons at 5 d.i.v. after immunostaining for SynCAM 1 (green) and tau (red). Specific SynCAM 1 staining is detected in growth cones. Boxes mark representative growth cones enlarged in the *Inset*. (D) SynCAM 1 is predominantly present on growth cone surfaces. Dissociated rat hippocampal neurons expressing extracellularly tagged SynCAM 1-pHluorin were imaged live at 5 d.i.v. at pH 7.4 (*Left*) and then transiently at pH 4 (*Center*) to quench the pHluorin surface signal. To detect the total pool of SynCAM 1-pHluorin, the same growth cone was permeabilized with 0.1% Triton X-100 containing fixative, washed, and imaged again at neutral pH using the same settings (*Right*). (E) Quantification of SynCAM 1-pHluorin fluorescence intensity obtained as in D ( $n = 3$ ).

dendritic contact triggers the threefold accumulation of SynCAM 1 at contacts within 5 min (Fig. 2*A–C* and *Movie S1*). No volumetric membrane increases occur at these sites (Fig. *S5*). Interestingly, SynCAM 1 assembly not only is initiated quickly, but also is completed rapidly, as its amount increases only marginally subsequent to contact (Fig. 2*B*,  $t_{45 \text{ min}}$ ). These SynCAM 1 assemblies persist once the growth cone migrates onward (Fig. 2*A*,  $t_{90 \text{ min}}$ ).

We next analyzed contacts between growth cones and neurites that both express SynCAM 1ΔIg1-pHluorin, a construct lacking the first Ig domain required for adhesion (14). This construct replicates the position of pHluorin in SynCAM 1-pHluorin and is expressed on growth cone surfaces (Fig. *S6*). Notably, this adhesion-deficient SynCAM 1 does not accumulate upon contact (Fig. 2*D* and *E*). Adhesive interactions therefore underlie the contact assembly of SynCAM 1.

To better define this assembly of SynCAM 1, we separately transfected neurons with SynCAM 1-pHluorin to detect it in

growth cones or with soluble Cherry to label neurites and cultured them together. Live imaging shows that SynCAM 1-pHluorin strongly accumulates in growth cones upon contact with Cherry-positive neurites (Fig. 2*F* and *G*). These results demonstrate that SynCAM 1 is a growth cone adhesion protein that assembles rapidly and stably at axo-dendritic contacts.

**Differentiation of SynCAM-Marked Axo-Dendritic Contact Sites.** We next asked whether SynCAM 1 assemblies mark differentiating growth cone contacts. Neurons were transfected with SynCAM 1-Cherry to detect it in growth cones or with GFP-tagged PSD-95 to label dendritic clusters, plated together, and analyzed (Fig. 2*H* and Fig. *S7*). Endogenous PSD-95 is already expressed at low levels in these immature neurons (see also Fig. 1*A*) and can be colocalized with the comparatively low number of developing synaptic contacts (26). Live imaging shows that growth cone filopodia containing SynCAM 1 are apposed to dendritic PSD-95 clusters. We frequently observed that these growth cone assemblies of SynCAM 1 remain juxtaposed to PSD-95-positive sites for hours (Fig. 2*H*), and we recorded the gradual accumulation of PSD-95 at these contacts (Fig. *S7*). These stable sites also contain other presynaptic proteins as shown by post-hoc immunostaining for synaptotagmin I (Fig. 2*I*). In consequence, discrete SynCAM 1 assemblies are retained along axonal crossing points with dendrites, and these sites remain stably apposed to PSD-95 clusters (Fig. 2*J*), with a subset containing presynaptic markers (Fig. 2*J*). Consistent with a continued differentiation of these sites, SynCAM 1 is localized to synapses in mature neurons (Fig. *S8*).

**SynCAM 1 Restricts the Structural Organization of Migrating Growth Cones.** Does SynCAM 1 function in growth cones before axo-dendritic contact? In support of morphogenetic roles, we observed that live growth cones containing elevated SynCAM 1 appear less dynamic than controls expressing myristoylated GFP (myrGFP) as a membrane marker (Fig. 3*A* and *B* and *Movie S2*). These optical recordings were acquired under nonlinear, high-gain conditions to trace the complete plasma membrane, unlike the analysis of SynCAM 1 localization under normal gain in Fig. 2. We first determined the number of growth cone filopodia that alter their length or position throughout the optical recording, scoring those as “active,” and show that elevated SynCAM 1 strongly reduces their number to  $48 \pm 11\%$  of control levels (Fig. 3*E*). We next determined the complexity of growth cones by Sholl analysis, an algorithm to assess the general complexity of structures (27). Because myrGFP and SynCAM 1-pHluorin delineate identical growth cone outlines (Fig. *S9A* and *B*), their comparative analysis was performed. This demonstrated that exogenous SynCAM 1-pHluorin lowers growth cone complexity to  $52 \pm 7\%$  of control levels (Fig. 3*F*), consistent with their simpler appearance. In agreement, exogenous SynCAM 1 reduces growth cone perimeters to  $49 \pm 16\%$  of control levels. SynCAM 1 is therefore sufficient to restrict growth cone filopodial dynamics and membrane complexity.

**SynCAM 1 Shapes Growth Cones Through FERM Interactions.** These morphogenetic roles of SynCAM 1 in growth cones pointed to interactions with cytoskeletal regulators. Such interactions can be mediated by an intracellular motif of SynCAMs predicted to bind FERM (protein 4.1/ezrin/radixin/moesin) domains (28) (Fig. 3*D*), which are present in a number of cytoskeletal components such as the SynCAM-binding partner protein 4.1B (29–31). To test this possibility, we generated a SynCAM 1ΔFERM-pHluorin mutant lacking five amino acids in this motif (Fig. 3*C* and *D*). This deletion prevents FERM domain interactions (see Fig. 4*A*) without altering SynCAM 1 expression in growth cone membranes as assessed from tracing studies (Fig. *S9C* and *D*). Interestingly, this ΔFERM mutation abrogates the effects of elevated SynCAM 1 on active filopodia number (Fig. 3*E*) and on





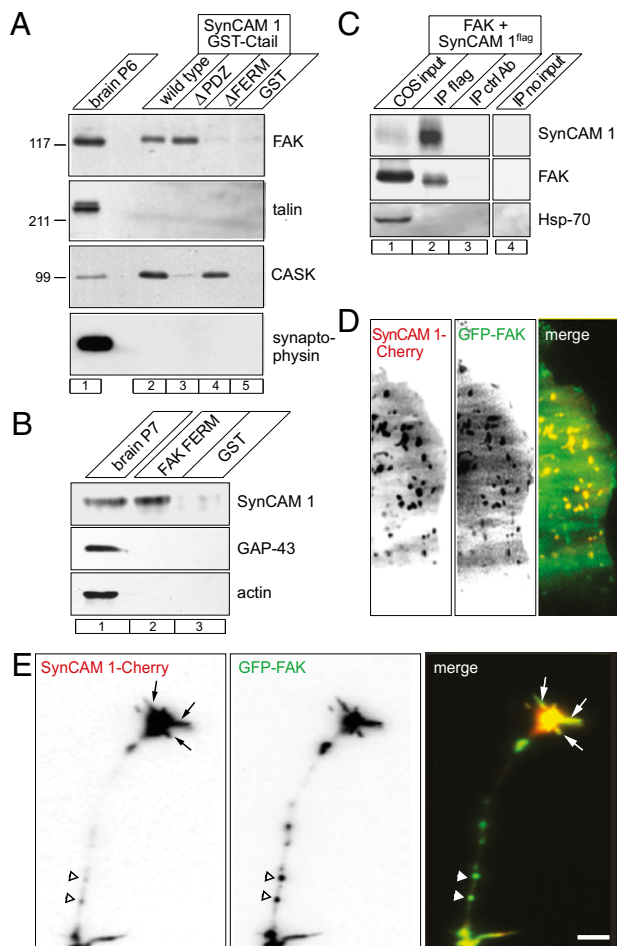


**Fig. 4.** FAK is a binding partner of SynCAM 1. (A) FAK binds the intracellular FERM motif of SynCAM 1. Rat forebrain proteins were solubilized at P5 and incubated with equal amounts of GST fusions of the cytosolic sequence of SynCAM 1, a  $\Delta$ PDZ construct, or its  $\Delta$ FERM mutant. GST served as control for nonspecific binding (lane 5). Eluate lanes contain  $1/40$  of the input shown. (B) Binding of SynCAM 1 to the FERM domain of FAK. Rat forebrain proteins extracted at P7 were bound to a GST fusion of the FERM domain of FAK, demonstrating SynCAM 1 retention. GAP-43 and actin served as negative controls, and GST as control for nonspecific binding. Eluate lanes contain  $1/50$  of the input shown. (C) Direct interaction of SynCAM 1 and FAK. Flag-tagged SynCAM 1 and FAK coexpressed in COS7 cells coimmunoprecipitate with anti-flag antibodies. Immunoprecipitates contain  $1/25$  of the input shown. (D) SynCAM 1 and FAK colocalize in the plasma membrane as imaged by TIRF microscopy of live COS7 cells coexpressing SynCAM 1-Cherry (red) and GFP-FAK (green). (E) TIRF microscopy of live rat hippocampal growth cones coexpressing GFP-FAK (green) and SynCAM 1-Cherry (red). The merged image shows their colocalization in the central growth cone region and its filopodia (arrows) and in apparent axonal transport packets (arrowheads). See [Movie S3](#). (Scale bar: 10  $\mu$ m.)

## Discussion

This study demonstrates that SynCAM 1 performs successive functions in developing neurons from shaping growth cones to the assembly of axo-dendritic contacts. These properties are distinct from other proteins like N-cadherin, which is mostly absent from growth cones and accumulates at synapses only after the growth cone has migrated on (39, 40), and are not shared by L1 and NCAM. These Ig proteins act in axon outgrowth and guidance (9), and SynCAM 1 additionally contributes to these growth-cone-dependent processes as axonal pathfinding errors occur when its expression is reduced in chicken (41). Although neuroligins have also been detected in growth cones (42), they have not been characterized in this compartment.

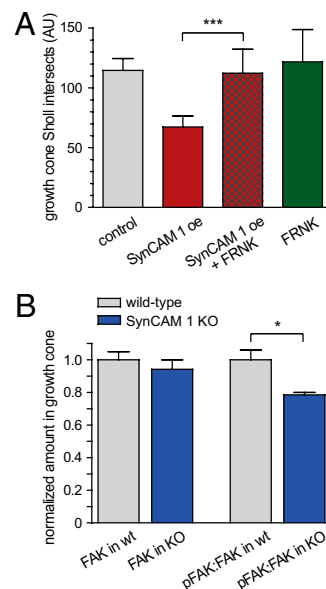


**Fig. 5.** FAK is a signaling partner of SynCAM 1. (A) Dominant-negative inhibition of FAK by FRNK blocks exogenous SynCAM 1-pHluorin from restricting complexity as shown by Sholl analysis (SynCAM 1-pH vs. SynCAM 1-pH plus FRNK,  $P = 0.001$ ;  $n = 4$ ). oe, overexpression. (B) Loss of SynCAM 1 reduces specific FAK activity in growth cones by  $22 \pm 6\%$  ( $P = 0.025$ ;  $n = 3$ ) while not affecting FAK enrichment in growth cones. Growth cones were prepared from wild-type and SynCAM 1 knockout mice at P7. Equal protein amounts were analyzed by quantitative immunoblotting for autophosphorylated and total FAK. Loaded amounts were normalized to GAP-43.

A key finding of this study is that SynCAM 1 assembles at growth cone contacts with target neurites. This likely involves its lateral clustering, but localized exocytosis may also contribute to its delivery to axo-dendritic contacts. We presume that SynCAM 1 clusters primarily engage in homophilic adhesion, as its heterophilic partner SynCAM 2 is less prominently expressed in the early postnatal hippocampus (16). SynCAM 2 expression increases in development, and its binding to SynCAM 1 could later refine these nascent sites. During these stages of synaptic differentiation, SynCAM adhesion may act in concert with other trans-synaptic adhesion molecules, such as neuroligins/neurexins (42–45).

Our study provides additional insight into the organization of migrating growth cones and finds that SynCAM 1 reduces the number of active filopodia. This is relevant as the regulation of filopodia by membrane proteins is insufficiently understood compared to the cytoskeletal machinery controlling these protrusions (46, 47). Interestingly, the restriction of active growth cone filopodia number by SynCAM 1 is converse to the postsynaptic effects of EphB receptors, which are required for proper dendritic filopodia motility (48). The expression levels of these membrane proteins may therefore mutually regulate the extent of axo-dendritic target exploration. Overall, this reduction in the membrane complexity of growth cones by elevated SynCAM 1 could result in their increased ability to maintain target contacts and differentiate them into synapses.

With respect to intracellular interactions, our results show that FAK is a binding partner and effector of SynCAM 1 in the shaping of migrating growth cones. This makes SynCAM 1 one of the few membrane proteins that directly bind FAK, together with EGF and PDGF receptors and possibly integrins (49, 50), NCAM 140 (51), and EphA receptors (52). FAK can be activated by engagement of its FERM domain (53), and SynCAM 1 binding may localize and spatially define FAK activity within growth cones. This would be consistent with the reduced specific FAK activity in growth cones lacking SynCAM 1. Interestingly, FAK restricts the

number of complex synapses in mature neurons (54), and future studies will determine whether a SynCAM–FAK complex operates at synapses subsequent to axo-dendritic contact.

## Materials and Methods

An extended section is provided in *SI Materials and Methods* and [Table S1](#).

**Biochemical Studies.** Rat forebrain homogenate was fractionated at P5–P7 (55). Affinity chromatography was performed as described (14).

**Neuronal Cell Culture.** Dissociated hippocampal neurons were cultured at postnatal day P0 or P1 (56). Mouse neuronal cultures were prepared from SynCAM 1 knockout mice (21) and compared to wild-type littermate controls.

**Live Imaging.** Neuronal cultures were imaged live at 5–6 d.i.v. in modified Tyrode solution (56) on an Olympus Ix81 microscope with an autofocus system

or on a Perkin-Elmer UltraView Spinning Disk microscope. TIRF imaging was performed on the Olympus Ix81 microscope. Images were obtained using a low-intensity laser line and low exposure to reduce phototoxicity.

Statistical analyses were performed using two-tailed *t* tests, and statistical errors correspond to SEM unless indicated otherwise.

**ACKNOWLEDGMENTS.** We thank Drs. A. Koleske, E. Stein, S. Strittmatter, and S. Chandra for discussions. We are grateful to Dr. T. Momoi (National Institute for Neuroscience, Tokyo) for generously providing SynCAM 1 knockout mice; Drs. C. Damsky (University of California at San Francisco) and D. Schlaepfer (University of California at San Diego) for FAK and FRNK vectors; Drs. B. Serrels and M. Frame (University of Edinburgh) for the GST–FAK FERM construct; Dr. D. Bredt (Lilly Research Laboratories) for the PSD-95 vector; and the Program in Cellular Neuroscience, Neurodegeneration and Repair, Yale University, for access to its imaging core. This work was supported by National Institutes of Health Grant R01 DA018928 (to T.B.), a Dana Foundation Brain and Immuno-Imaging Grant (to T.B.), and a Brown-Coxe Fellowship (to M.S.).

- Cooper MW, Smith SJ (1992) A real-time analysis of growth cone-target cell interactions during the formation of stable contacts between hippocampal neurons in culture. *J Neurobiol* 23:814–828.
- Ziv NE, Smith SJ (1996) Evidence for a role of dendritic filopodia in synaptogenesis and spine formation. *Neuron* 17:91–102.
- Fiala JC, Feinberg M, Popov V, Harris KM (1998) Synaptogenesis via dendritic filopodia in developing hippocampal area CA1. *J Neurosci* 18:8900–8911.
- Rees RP, Bunge MB, Bunge RP (1976) Morphological changes in the neuritic growth cone and target neuron during synaptic junction development in culture. *J Cell Biol* 68:240–263.
- Ahmari SE, Smith SJ (2002) Knowing a nascent synapse when you see it. *Neuron* 34:333–336.
- Jin Y, Garner CC (2008) Molecular mechanisms of presynaptic differentiation. *Annu Rev Cell Dev Biol* 24:237–262.
- Lowery LA, Van Vactor D (2009) The trip of the tip: Understanding the growth cone machinery. *Nat Rev Mol Cell Biol* 10:332–343.
- Pak CW, Flynn KC, Bamberg JR (2008) Actin-binding proteins take the reins in growth cones. *Nat Rev Neurosci* 9:136–147.
- Maness PF, Schachner M (2007) Neural recognition molecules of the immunoglobulin superfamily: Signaling transducers of axon guidance and neuronal migration. *Nat Neurosci* 10:19–26.
- Suter DM, Errante LD, Belotserkovsky V, Forscher P (1998) The Ig superfamily cell adhesion molecule, apCAM, mediates growth cone steering by substrate-cytoskeletal coupling. *J Cell Biol* 141:227–240.
- Dalva MB, McClelland AC, Kayser MS (2007) Cell adhesion molecule: Signalling functions at the synapse. *Nat Rev Neurosci* 8:206–220.
- Biederer T, Stagi M (2008) Signaling by synaptogenic molecules. *Curr Opin Neurobiol* 18:261–269.
- Arikath J, Reichardt LF (2008) Cadherins and catenins at synapses: Roles in synaptogenesis and synaptic plasticity. *Trends Neurosci* 31:487–494.
- Biederer T, et al. (2002) SynCAM, a synaptic adhesion molecule that drives synapse assembly. *Science* 297:1525–1531.
- Shingai T, et al. (2003) Implications of nectin-like molecule-2/IGSF4/RA175/SgIGSF/TSLC1/SynCAM1 in cell-cell adhesion and transmembrane protein localization in epithelial cells. *J Biol Chem* 278:35421–35427.
- Thomas LA, Akins MR, Biederer T (2008) Expression and adhesion profiles of SynCAM molecules indicate distinct neuronal functions. *J Comp Neurol* 510:47–67.
- Fogel AI, et al. (2007) SynCAMs organize synapses through heterophilic adhesion. *J Neurosci* 27:12516–12530.
- Kang Y, Zhang X, Dobie F, Wu H, Craig AM (2008) Induction of GABAergic postsynaptic differentiation by alpha-neurexins. *J Biol Chem* 283:2323–2334.
- Song JY, Ichtchenko K, Südhof TC, Brose N (1999) Neuroligin 1 is a postsynaptic cell-adhesion molecule of excitatory synapses. *Proc Natl Acad Sci USA* 96:1100–1105.
- Dotti CG, Sullivan CA, Banker GA (1988) The establishment of polarity by hippocampal neurons in culture. *J Neurosci* 8:1454–1468.
- Fujita E, et al. (2006) Oligo-astheno-teratozoospermia in mice lacking RA175/TSLC1/SynCAM/IGSF4, a cell adhesion molecule in the immunoglobulin superfamily. *Mol Cell Biol* 26:718–726.
- Nozumi M, et al. (2009) Identification of functional marker proteins in the mammalian growth cone. *Proc Natl Acad Sci USA* 106:17211–17216.
- Miesenböck G, De Angelis DA, Rothman JE (1998) Visualizing secretion and synaptic transmission with pH-sensitive green fluorescent proteins. *Nature* 394:192–195.
- Meyer MP, Smith SJ (2006) Evidence from in vivo imaging that synaptogenesis guides the growth and branching of axonal arbors by two distinct mechanisms. *J Neurosci* 26:3604–3614.
- Ahmari SE, Buchanan J, Smith SJ (2000) Assembly of presynaptic active zones from cytoplasmic transport packets. *Nat Neurosci* 3:445–451.
- Anderson TR, Shah PA, Benson DL (2004) Maturation of glutamatergic and GABAergic synapse composition in hippocampal neurons. *Neuropharmacology* 47:694–705.
- Sholl DA (1953) Dendritic organization in the neurons of the visual and motor cortices of the cat. *J Anat* 87:387–406.
- Biederer T (2006) Bioinformatic characterization of the SynCAM family of immunoglobulin-like domain-containing adhesion molecules. *Genomics* 87:139–150.
- Hoy J, Constable J, Vicini S, Fu Z, Washbourne P (2009) SynCAM1 recruits NMDA receptors via protein 4.1B. *Mol Cell Neurosci* vol 42:466–483.
- Diakowski W, Grzybek M, Sikorski AF (2006) Protein 4.1, a component of the erythrocyte membrane skeleton and its related homologue proteins forming the protein 4.1/FERM superfamily. *Folia Histochem Cytobiol* 44:231–248.
- Chishti AH, et al. (1998) The FERM domain: A unique module involved in the linkage of cytoplasmic proteins to the membrane. *Trends Biochem Sci* 23:281–282.
- Burgaya F, Menegon A, Menegoz M, Valtorta F, Girault JA (1995) Focal adhesion kinase in rat central nervous system. *Eur J Neurosci* 7:1810–1821.
- Chan KT, Cortesio CL, Huttenlocher A (2009) FAK alters invadopodia and focal adhesion composition and dynamics to regulate breast cancer invasion. *J Cell Biol* 185:357–370.
- Robles E, Gomez TM (2006) Focal adhesion kinase signaling at sites of integrin-mediated adhesion controls axon pathfinding. *Nat Neurosci* 9:1274–1283.
- Mitra SK, Hanson DA, Schlaepfer DD (2005) Focal adhesion kinase: In command and control of cell motility. *Nat Rev Mol Cell Biol* 6:56–68.
- Parsons JT, Martin KH, Slack JK, Taylor JM, Weed SA (2000) Focal adhesion kinase: A regulator of focal adhesion dynamics and cell movement. *Oncogene* 19:5606–5613.
- Richardson A, Parsons T (1996) A mechanism for regulation of the adhesion-associated protein tyrosine kinase pp125FAK. *Nature* 380:538–540.
- Schaller MD, Borgman CA, Parsons JT (1993) Autonomous expression of a noncatalytic domain of the focal adhesion-associated protein tyrosine kinase pp125FAK. *Mol Cell Biol* 13:785–791.
- Benson DL, Tanaka H (1998) N-cadherin redistribution during synaptogenesis in hippocampal neurons. *J Neurosci* 18:6892–6904.
- Jontes JD, Emond MR, Smith SJ (2004) In vivo trafficking and targeting of N-cadherin to nascent presynaptic terminals. *J Neurosci* 24:9027–9034.
- Niederkofler V, Baeriswyl T, Ott R, Stoekli ET (2010) Nectin-like molecules/SynCAMs are required for post-crossing commissural axon guidance. *Development* 137:427–435.
- Dean C, et al. (2003) Neurexin mediates the assembly of presynaptic terminals. *Nat Neurosci* 6:708–716.
- Nam CI, Chen L (2005) Postsynaptic assembly induced by neurexin-neuroigin interaction and neurotransmitter. *Proc Natl Acad Sci USA* 102:6137–6142.
- Gerrow K, et al. (2006) A preformed complex of postsynaptic proteins is involved in excitatory synapse development. *Neuron* 49:547–562.
- Graf ER, Zhang X, Jin S-X, Linhoff MW, Craig AM (2004) Neurexins induce differentiation of GABA and glutamate postsynaptic specializations via neuroligins. *Cell* 119:1013–1026.
- Gupton SL, Gertler FB (2007) Filopodia: The fingers that do the walking. *Sci STKE* 2007:re5.
- Faix J, Rottner K (2006) The making of filopodia. *Curr Opin Cell Biol* 18:18–25.
- Kayser MS, Nolt MJ, Dalva MB (2008) EphB receptors couple dendritic filopodia motility to synapse formation. *Neuron* 59:56–69.
- Sieg DJ, et al. (2000) FAK integrates growth-factor and integrin signals to promote cell migration. *Nat Cell Biol* 2:249–256.
- Schaller MD, Otey CA, Hildebrand JD, Parsons JT (1995) Focal adhesion kinase and paxillin bind to peptides mimicking beta integrin cytoplasmic domains. *J Cell Biol* 130:1181–1187.
- Beggs HE, Baragona SC, Hemperly JJ, Maness PF (1997) NCAM140 interacts with the focal adhesion kinase p125(fak) and the SRC-related tyrosine kinase p59(fyn). *J Biol Chem* 272:8310–8319.
- Miao H, Burnett E, Kinch M, Simon E, Wang B (2000) Activation of EphA2 kinase suppresses integrin function and causes focal-adhesion-kinase dephosphorylation. *Nat Cell Biol* 2:62–69.
- Dunty JM, et al. (2004) FERM domain interaction promotes FAK signaling. *Mol Cell Biol* 24:5353–5368.
- Rico B, et al. (2004) Control of axonal branching and synapse formation by focal adhesion kinase. *Nat Neurosci* 7:1059–1069.
- Phelan P, Gordon-Weeks R (1997) *Isolation of Synaptosomes, Growth Cones, and Their Subcellular Components* (Oxford University Press, Oxford), pp 1–38.
- Biederer T, Scheiffele P (2007) Mixed-culture assays for analyzing neuronal synapse formation. *Nat Protoc* 2:670–676.

# Supporting Information

Stagi et al. 10.1073/pnas.0911798107

## SI Materials and Methods

**Antibodies.** For immunolocalization in dissociated neurons, antibodies were employed against SynCAM 1 (MBL Laboratories; clone 3E1, 1:500) and the axonal marker tau (Chemicon; MAB3420, 1:500). For detection of synaptic markers, antibodies were employed against synaptotagmin I (Synaptic Systems; clone 41.1, 1:100) and SV2 (developed by Kathleen Buckley, 1:500; obtained from the Developmental Studies Hybridoma Bank maintained by the University of Iowa).

Immunoblotting was performed with specific SynCAM 1 antibodies reported previously (1) (all 1:1000). Immunoblotting was additionally performed with monoclonal antibodies raised in mouse against FAK (Millipore; clone 4.47, 1:1,000), phospho-FAK to detect activated FAK phosphorylated at Tyr397 (2) (Millipore; MAB1144, 1:1,000), neuroligin 1 (Synaptic Systems; clone 4C12.1, 1:2,500, CASK (NeuroMab; clone K56A/50, 1:1,000), synaptophysin (Synaptic Systems; clone Cl604.4, 1:5000), synaptotagmin I (Synaptic Systems; clone Cl604.1, 1:1,000), and actin (MP Biomedical; clone C4 69100, 1:5000). Polyclonal antibodies used for immunoblotting were raised in rabbits against neurexin (Synaptic Systems; 1:1000) and PSD-95 (Synaptic Systems; 1:2,000). Antibodies raised in mouse against talin (Chemicon; MAB3264, 1:500) were a gift from Pietro De Camilli (Department of Cell Biology, Yale University), antibodies against Hsp-70 (Santa Cruz Biotechnology; clone 3A3, 1:200) were from Antony Koleske (Department of Molecular Biophysics and Biochemistry, Yale University), and antibodies against GAP-43 (Abcam; clone 7B10, 1:500) were a gift from Karina Meiri (Department of Anatomy and Cellular Biology, Tufts University). Antibodies raised in mouse against DCC (Pharmingen; clone 15041A; Calbiochem; clone OP45; used in combination at each 0.5  $\mu\text{g}/\text{mL}$ ) were a gift from Elke Stein (Department of Molecular, Cellular, and Developmental Biology, Yale University). Immunoprecipitation was performed with anti-flag monoclonal antibodies (Sigma; M2, 1:50).

**Vector Construction.** Sequences of primers and PCR templates used for vector construction are provided in Table S1. All vectors generated in this study were sequenced to verify correct insertion. Correct protein expression from all eukaryotic expression vectors used in this study was confirmed by fluorescence microscopy and immunoblotting in HEK 293 and COS7 cells after transfection using FuGENE 6 (Roche Applied Science).

The SynCAM 1 expression vector pCAGGS SynCAM1 was generated by subcloning full-length mouse SynCAM 1 (splice product 4; ref. 3) using EcoRI from pCMV5-SynCAM1 (4) into the vector pCAGGS (a gift from Jun-ichi Miyazaki, Osaka University) (5). To generate SynCAM 1 constructs with extracellular insertion of a fluorescent protein carboxyl-terminal of the third Ig domain, the vector pCAGGSSynCAM1(363)\*NheI was generated from pCAGGS-SynCAM1 by PCR mutagenesis using the oligo pair TB127/MS027. The number in parentheses indicates the amino acid into the codon of which the restriction site was introduced. To generate the vector pCAGGS-SynCAM1(363)\*NheI- $\Delta\text{Ig1}$ , pCAGGS-SynCAM1(363)\*NheI was digested with BmgBI and EcoRV to remove the sequence encoding amino acids 54–159 and religated. To generate the pCAGGS-SynCAM1(363)\*NheI- $\Delta\text{FERM}$  construct, two fragments were generated by PCR from pCAGGSSynCAM1(363)\*NheI using the oligo pairs MS029/LS001 and LS002/TB139, ligated using SalI, and subcloned into pCAGGS. Sequences encoding fluorescent proteins were amplified by PCR from pRSETB-Cherry

(a gift from Roger Tsien, University of California, San Diego) and pCI neo synaptotHluorin (a gift from Dr. James Rothman, Yale University, New Haven, CT) using oligos TB123/TB124, subcloned into pCR-BluntII-TOPO (Invitrogen) to generate Cherry and pHluorin cloning vectors, and inserts were subcloned using NheI in the expression vectors pCAGGS-SynCAM1(363)\*NheI, pCAGGSSynCAM1(363)\*NheI- $\Delta\text{FERM}$ , or pCAGGS SynCAM1(363)\*NheI- $\Delta\text{Ig1}$ . The pCAGGS-SynCAM1(363)flag vector was described previously (1).

The pCAGGS-myrGFP vector was generated by PCR amplifying the insert from pSRC-myrEGFP (a gift from Mikhail Khvotchev and Thomas Südhof, University of Texas Southwestern Medical Center, and Stanford University) using the oligo pair MS047/MS048, cloning the product into pCR-BluntII-TOPO, and subcloning the insert after partial EcoRI digest into pCAGGS. pCAGGS-myrCherry was generated by first PCR amplifying the sequence encoding Cherry from pRSETB-Cherry using the oligo pair TB123/MS052, cloning the product into pCR-BluntII-TOPO, subcloning the insert into pCAGGS using EcoRI to generate pCAGGS-Cherry, amplifying the myristoylation sequence from pSRC-myrEGFP using oligo pairs TB148/TB149, and subcloning the myristoylation sequence into pCAGGS-Cherry using a 5' NheI site. pCAGGS-myrpHluorin was generated by PCR amplifying the sequence encoding pHluorin from the pRSETB-pHluorin vector using oligos MS072 and MS073, followed by the steps described for pCAGGS-myrGFP.

To generate the vectors pCAGGS-GFP-FAK and pCAGGS-GFP-FRNK, the sequences encoding GFP-FAK and GFP-FRNK were PCR amplified from pEGFP-C1-FAK and pEGFP-C1-FRNK (6) [gifts of Caroline Damsky (San Francisco) and David Schlaepfer (San Diego)] using the oligo pairs TB123/MS063 and TB123/MS061, respectively. The GFP-FAK product was subcloned into a modified pCAGGS vector using NheI. The GFP-FRNK product was cloned into pCR-BluntII-TOPO and then subcloned into pCAGGS using EcoRI. To generate pCAGGS-PSD95GFP, PSD-95 tagged N-terminally with GFP was amplified by PCR with the oligo pair MS064/MS065 from pGW1CMV PSD95-eGFP (a gift of David Bredt, Indianapolis), and the product was cloned into a modified pCAGGS vector using an NheI site.

To generate GST-fusion proteins of the SynCAM 1 cytosolic sequences corresponding to the wild-type form or the variant lacking the PDZ interaction motif, the constructs pGEXKG-SynCAM1Ctail and pGEXKGSynCAM1Ctail $\Delta\text{PDZ}$  were obtained by generating PCR products from pCMV-SynCAM 1 with oligos DA001/DA002 and DA001/DA003, respectively, digesting with Asp781 and NotI, filling in, and subcloning using SmaI in pGEXKG. pGEXKG-SynCAM1Ctail $\Delta\text{FERM}$  was generated by PCR amplification of a product from pCAGGS-SynCAM 1 with oligos TB145/139, and subcloning it using SmaI/HindIII in pGEXKG. The vector pGEXKG-neurexin I was described previously (7). The vector pGEX6P3 FAK FERM37-378 (8) was a gift from Bryan Serrels and Margaret Frame (Edinburgh).

**Biochemical Studies.** For expression profiling in hippocampal neurons, neurons were plated at a density of  $1 \times 10^6$  cells  $\text{mL}^{-1}$ , and lysates were collected at 5 and 16 days in vitro (d.i.v.) in lysis buffer containing protease inhibitors. Rat forebrain homogenate was fractionated at postnatal days P5–P7 by the differential centrifugation method of Gordon-Weeks and Lockerbie to isolate preparations containing growth cones (9). For analysis of FAK phosphorylation, phosphatase inhibitors were included

in this fractionation (1 mM Na<sub>3</sub>VO<sub>4</sub>, 50 mM NaF, 10 mM  $\beta$ -glycerolphosphate, and 10 mM sodium pyrophosphate).

For affinity chromatography on GST fusion proteins, rat forebrain homogenate was prepared from P5–P7 animals in homogenization buffer (25 mM Hepes–NaOH, pH 7.4, 25 mM potassium acetate, 320 mM sucrose) in the presence of protease inhibitors [1 mg/L pepstatin, 1 mg/L aprotinin, 10 mg/L leupeptin (all from Roche Applied Science), 0.5 mM PMSF (Sigma), and phosphatase inhibitors (1 mM Na<sub>3</sub>VO<sub>4</sub>, 2 mM  $\beta$ -glycerol phosphate, 10 mM NaF, 2 mM sodium pyrophosphate)], and centrifuged to obtain the postnuclear supernatant. The postnuclear supernatant was adjusted to 1.0% Triton X-100 (Roche Applied Science), centrifuged in a Beckman Optima TLX centrifuge using the rotor TLA 100.3 at 60,000 rpm for 30 min at 4 °C, and the supernatant was precleared on glutathione agarose (GE Healthcare) for 2 h at 4 °C. As affinity matrix, GST fusion proteins were expressed and purified in *Escherichia coli* as described (4, 7). Detergent extracts were then loaded onto these beads, incubated overnight at 4 °C, and washed with ice-cold binding buffer, and bound proteins were eluted with 2% SDS.

Immunoprecipitation of flag-tagged SynCAM 1 was performed from transfected COS7 cells solubilized in homogenization buffer with 1.0% Triton X-100 (Roche Applied Science) and subjected to immunoprecipitation with anti-flag antibodies (Sigma; M2, 1:50). Protein concentrations were determined using the Pierce BCA assay. SDS–polyacrylamide gel electrophoresis and immunoblotting were performed using standard procedures.

**Immunocytochemistry.** Images were acquired on a Zeiss LSM 510 META laser scanning confocal microscope, with channels scanned separately to avoid signal contamination and a pinhole set to 1  $\mu$ m for each channel. Images were acquired using the LSM software package (Zeiss). For the detection of endogenous SynCAM 1 in growth cones, dissociated rat neuronal cultures were fixed at 5 d.i.v. with 4% paraformaldehyde/4% sucrose in PBS, washed extensively in PBS, blocked in 5% BSA/0.1% Triton-X100 in PBS, and probed with anti-SynCAM 1 antibodies (MBL Laboratories; clone 3E1, 1:500) for 2 h at room temperature, followed by extensive washes before detection with secondary antibodies.

**Neuronal Cell Culture.** Dissociated rat and mouse hippocampal neurons were cultured from pups at postnatal days P0 or P1 as described (10) and grown on Matrigel (Becton-Dickinson Biosciences). Mouse neuronal cultures were prepared from SynCAM 1 knockout mice generously provided by Takashi Momoi (National Institute of Neuroscience, Tokyo) (11) and compared to wild-type littermate controls. Neurons were transfected using electroporation at the time of dissociation using an Amaxa Nucleofactor system, following the manufacturer's instructions.

**Live Imaging of Growth Cones and Axo-Dendritic Contacts.** Neuronal cultures were imaged live at 5–6 d.i.v. in modified Tyrode solution (10). Growth cones were identified on the basis of their splayed morphology. To analyze the effects of SynCAM 1 on the organization of migrating growth cones, growth cones that were physically isolated from neurons and glia were selected. Images were acquired on an inverted, motorized Olympus Ix81 microscope equipped with a cooled, highly linear Andor iXon camera and an OlympusIX2-UCB autofocus system with a microscope stage heated to 37 °C, except for the quenching studies as described below.

For analyses of filopodial dynamics and growth cone complexity, this TIRF-equipped setup was used in a non-TIRF, epifluorescence-like mode after decreasing the light entry beyond the critical angle. This generated a deep evanescent field of low phototoxicity for entire illumination of the imaged growth cones and neurites [optical thickness in epifluorescence-like mode equal to or greater than 500 nm, which is sufficient to illuminate the entire growth cone volume due to their average thickness of  $\approx$ 260 nm

(12)]. All images were obtained using autofocus, a low-intensity laser line and short exposure to additionally reduce phototoxicity, and at high gain to detect all fluorescence throughout the overexpressing growth cones. Filopodia were identified as elongated, thin protrusions extending from the growth cone anterior to its base that have an even diameter throughout and a length:diameter ratio of at least 4. Such protrusions were scored as active filopodia if they translocated in space or extended or shortened their length between each frame for the full imaging period indicated in the figure legends. The vast majority of filopodia observed on growth cones was scored as active.

Sholl analysis (13) of growth cone complexity was performed for each frame of the acquired movies using a custom-written Matlab script (MathWorks). Briefly, the growth cone was placed in the center of each frame, and Sholl analysis was applied from the center of the growth cone to the periphery. The cumulative score for each successive frame was then plotted to provide a measure of growth cone complexity over time. SynCAM 1 knockout mouse neurons were compared in these experiments to wild-type littermate controls, and rescue studies with SynCAM 1 were performed in knockout mouse neurons after electroporation at the time of plating. All other overexpression studies were performed in dissociated rat hippocampal neurons that were electroporated as described above. Growth cone perimeters were analyzed using a custom Matlab script for Sholl analyses.

To examine surface interactions of growth cones with dendrites, dissociated hippocampal neurons were electroporated with single expression vectors and mixed at 1:1 cell density before plating where indicated. Live movies were acquired using the Olympus Ix81 setup described above, which was equipped with an Andor iXon camera and an autofocus system with a microscope stage heated to 37 °C. Images were acquired in an epifluorescence-like mode to illuminate the entire growth cone and dendrite volume at a rate of one frame every 5 min over periods of 3–5 h. Axons were distinguished from dendrites by their narrow diameter, their extension far from the cell body, and the presence of a splayed growth cone. Line scan analyses were performed using ImageJ.

**Total Internal Reflection Fluorescence Imaging.** Cells were imaged live in modified Tyrode solution, and live images were acquired on an inverted, motorized Olympus Ix81 microscope equipped with a cooled, highly linear Andor iXon camera and an OlympusIX2-UCB autofocus system with a microscope stage heated to 37 °C. Images were acquired in total internal reflection fluorescence (TIRF) mode to illuminate and analyze membrane-proximal areas (optical thickness of  $\sim$ 250 nm). Images were obtained using a low-intensity laser line and low exposure to reduce phototoxicity.

**Live Imaging of pHluorin Quenching.** For quantitative analysis of the surface expression of exogenous SynCAM 1, hippocampal neurons expressing SynCAM 1–pHluorin were imaged at 5 d.i.v. at room temperature in modified Tyrode solution (pH 7.4) on a Perkin-Elmer UltraView VoX Spinning Disk microscope equipped with a Hamamatsu C9100-50 camera and a Nikon Perfect Focus autofocus system, set to a resolution of 0.120  $\mu$ m/pixel, and acquired at 153 ms/frame. A growth cone was randomly selected, and imaging was continued for 55 s. The pH of the medium was then rapidly lowered by replacing the medium with modified Tyrode solution (pH 4.0, adjusted with HCl) using a perfusion system (AutoMate Scientific; ValveLink 8.2). Imaging was continued for 40 s to determine the extent of quenching of the extracellular pHluorin tag by low pH. The pH of the medium was then readjusted by perfusion with modified Tyrode solution (pH 8) while imaging was continued.

**Miscellaneous Procedures.** Statistical analyses were performed using two-tailed *t* tests, and statistical errors stated in the text and figure legends correspond to the standard error of the mean

unless otherwise indicated. Statistical analyses were performed using GraphPad Prism. Matlab scripts used for image analyses are available upon request. All animal procedures undertaken in

this study were approved by the Yale University Institutional Animal Care and Use Committee and were in compliance with National Institutes of Health guidelines.

1. Fogel AI, et al. (2007) SynCAMs organize synapses through heterophilic adhesion. *J Neurosci* 27:12516–12530.
2. Chan PY, Kanner SB, Whitney G, Aruffo A (1994) A transmembrane-anchored chimeric focal adhesion kinase is constitutively activated and phosphorylated at tyrosine residues identical to pp125FAK. *J Biol Chem* 269:20567–20574.
3. Biederer T (2006) Bioinformatic characterization of the SynCAM family of immunoglobulin-like domain-containing adhesion molecules. *Genomics* 87:139–150.
4. Biederer T, et al. (2002) SynCAM, a synaptic adhesion molecule that drives synapse assembly. *Science* 297:1525–1531.
5. Niwa H, Yamamura K, Miyazaki J (1991) Efficient selection for high-expression transfectants with a novel eukaryotic vector. *Gene* 108:193–199.
6. Ilić D, et al. (1998) Extracellular matrix survival signals transduced by focal adhesion kinase suppress p53-mediated apoptosis. *J Cell Biol* 143:547–560.
7. Biederer T, Südhof TC (2000) Mints as adaptors. Direct binding to neuexins and recruitment of munc18. *J Biol Chem* 275:39803–39806.
8. Serrels B, et al. (2007) Focal adhesion kinase controls actin assembly via a FERM-mediated interaction with the Arp2/3 complex. *Nat Cell Biol* 9:1046–1056.
9. Phelan P, Gordon-Weeks R (1997) *Isolation of Synaptosomes, Growth Cones, and Their Subcellular Components* (Oxford University Press, Oxford), pp 1–38.
10. Biederer T, Scheiffele P (2007) Mixed-culture assays for analyzing neuronal synapse formation. *Nat Protoc* 2:670–676.
11. Fujita E, et al. (2006) Oligo-astheno-teratozoospermia in mice lacking RA175/TS1C1-SynCAM/IGSF4A, a cell adhesion molecule in the immunoglobulin superfamily. *Mol Cell Biol* 26:718–726.
12. McNally HA, Rajwa B, Sturgis J, Robinson JP (2005) Comparative three-dimensional imaging of living neurons with confocal and atomic force microscopy. *J Neurosci Methods* 142:177–184.
13. Sholl DA (1953) Dendritic organization in the neurons of the visual and motor cortices of the cat. *J Anat* 87:387–406.
14. Hata Y, Davletov B, Petrenko AG, Jahn R, Südhof TC (1993) Interaction of synaptotagmin with the cytoplasmic domains of neuexins. *Neuron* 10:307–315.



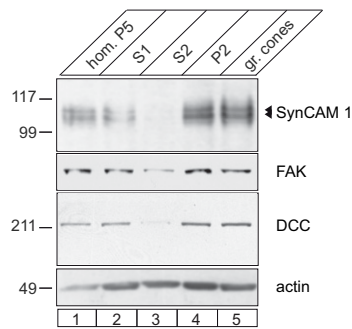


**Fig. S2.** SynCAM 1 cofractionation with growth cones. Growth cones were prepared by subcellular fractionation from rat brain at P5 and analyzed by immunoblotting. SynCAM 1 was detected with the specific antibody YUC8. FAK and the growth cone protein DCC served as fractionation controls, and actin as loading control. Hom., total brain homogenate; S1, postnuclear supernatant; S2, cytosolic fraction; P2, membrane pellet; gr. cones, crude growth cone fraction.

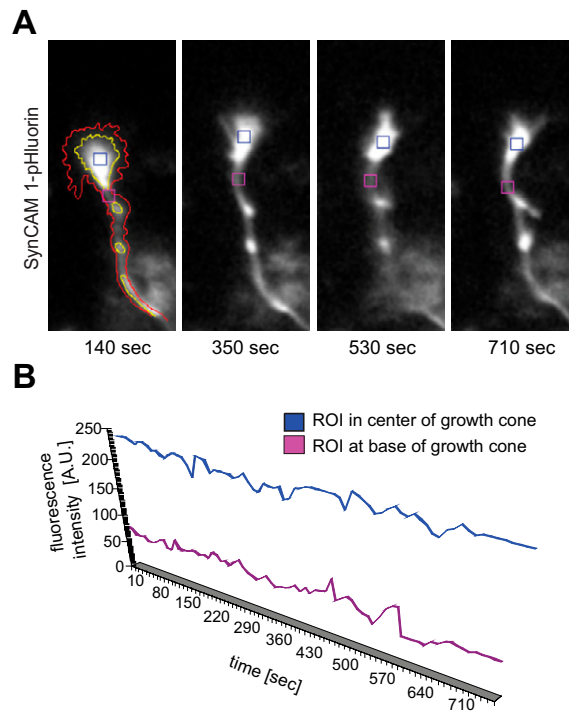


**Fig. S3.** Expression of exogenous SynCAM 1 in growth cones. (A) Live imaging of dissociated rat hippocampal neurons expressing SynCAM 1-pHluorin demonstrates its presence in the central region of growth cones and filopodial protrusions. Panels correspond to consecutive frames of the same field of view taken at the indicated time points over a total imaging period of 750 s. In the first panel, the red trace outlines the growth cone perimeter and the yellow trace the central area exhibiting elevated SynCAM 1-pHluorin intensity. The red trace was determined identically as for the Sholl analyses in the main text. Blue and violet squares indicate regions of interest (ROI) in growth cone central regions and neurite base, respectively, that were selected for the analysis of SynCAM 1-pHluorin distribution in B. (B) Quantitative analysis of the recording in A demonstrates a threefold enrichment of exogenous SynCAM 1-pHluorin in the central region of migrating growth cones relative to the neurite base of the growth cones. Analyzed ROI are marked in A. The differential distribution remains constant as the growth cone migrates. The graph shows the analysis for each frame obtained every 10 s during the observation period of 750 s.

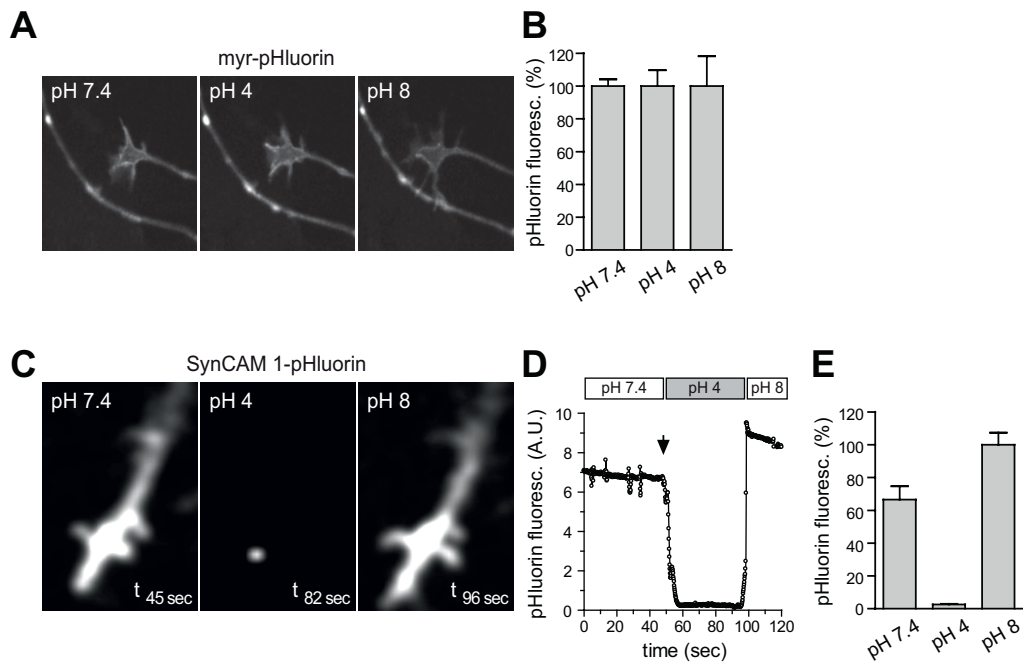


**Fig. S4.** Surface expression analysis of SynCAM 1-pHluorin in growth cones. (A) A myristoylated pHluorin construct (myr-pHluorin) is not sensitive to acidification of the extracellular medium. Growth cones of dissociated rat hippocampal neurons expressing myr-pHluorin were imaged live at 5 d.i.v. at pH 7.4 (Left) and then during transient lowering of the extracellular medium to pH 4 (Center). The fluorescence intensity of the myr-pHluorin signal is not quenched by transient lowering of the extracellular pH and remains unchanged after subsequent extracellular neutralization (Right), consistent with the absence of membrane permeabilization and intracellular acidification at pH 4. Note that the growth cone contacts a target neurite during the imaging period. (B) Quantification of myr-pHluorin fluorescence intensity during transient lowering of the extracellular pH as shown in A.  $n = 3$  growth cones. (C) SynCAM 1 tagged with pH-sensitive pHluorin is present on growth cone surfaces. Dissociated hippocampal rat neurons expressing SynCAM 1-pHluorin were imaged live at 5 d.i.v. at pH 7.4 (Left) and then transiently at pH 4 (Center) as in A. Low pH quenches the SynCAM 1-pHluorin signal almost completely from growth cones, but is fully recovered after extracellular neutralization (Right). (D) The graph shows the extent of fluorescence loss and recovery in C, with the arrow marking the start of quenching. The postquenching fluorescence signal is higher as the neutralizing buffer had pH 8, allowing for a greater quantum yield of pHluorin than at pH 7.4. (E) Quantification of SynCAM 1-pHluorin fluorescence intensity during transient lowering of the extracellular pH as shown in C and D.  $n = 4$  growth cones.

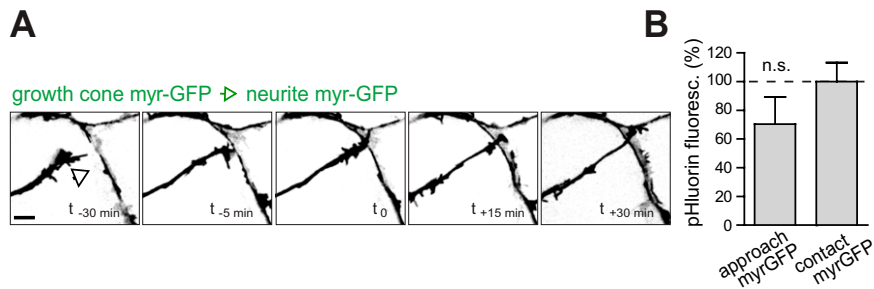


**Fig. S5.** Absence of membrane accumulation upon growth cone contact. (A) Dissociated rat hippocampal growth cones expressing the control protein myr-GFP that is targeted to the intracellular leaflet of the plasma membrane were imaged at 5 d.i.v. as they advanced toward a dendrite. The arrowhead marks the growth cone direction. Frames were obtained every 5 min. (Scale bar: 10  $\mu$ m.) (B) Axo-dendritic contact does not increase myr-GFP intensity at the site of contact, consistent with a lack of membrane accumulation. Fluorescence intensities were determined after line scan analysis as described in Fig. 2B of the main text before and during contact (two-tailed  $t$  test) n.s., not significant.  $n = 3$  growth cones.

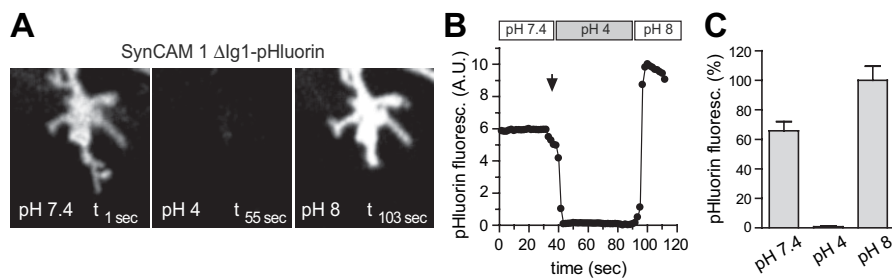


**Fig. S6.** Surface expression of SynCAM 1  $\Delta$ Ig1-pHluorin in growth cones. (A) Dissociated rat hippocampal neurons expressed SynCAM 1  $\Delta$ Ig1-pHluorin, a construct lacking the first Ig domain required for adhesive binding, and were imaged live at 5 d.i.v. at pH 7.4 (*Left*) and then transiently at pH 4 (*Center*). Low pH quenches the SynCAM 1  $\Delta$ Ig1-pHluorin signal almost completely from growth cones, consistent with its surface expression. This is fully reversible by extracellular neutralization (*Right*). (B) The graph shows the extent of fluorescence loss and recovery in A, with the arrow marking the start of quenching. For an explanation of the increased postquenching fluorescence signal, see the legend of Fig. S4D. (C) Quantification of SynCAM 1  $\Delta$ Ig1-pHluorin fluorescence intensity during transient lowering of the extracellular pH as shown in A and B.  $n = 4$  growth cones. Note that the same results were obtained for SynCAM 1  $\Delta$ Ig1-pHluorin as for SynCAM 1-pHluorin in Fig. S4E.

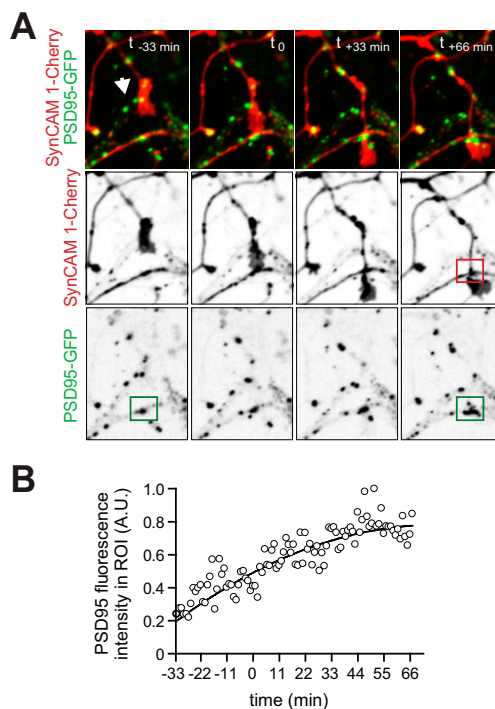


**Fig. S7.** Postsynaptic assembly at contacts of SynCAM 1-marked growth cones. (A) Dissociated rat hippocampal neurons were separately transfected with SynCAM 1-Cherry (red) or PSD95-GFP (green), cultured together, and imaged live at 5 d.i.v. on a Perkin-Elmer UltraView VoX Spinning Disk microscope. Images were acquired at 1 frame every 1 min for a total acquisition period of 99 min. Panels depict the same field of view, with merged images in the top row, and the SynCAM 1-Cherry and PSD95-GFP channels in the second and third rows, respectively.  $t_0$  marks the frame when contact between the SynCAM 1-expressing growth cone and a PSD95-GFP positive dendrite occurred. PSD95-GFP positive puncta migrate progressively over time to this point of contact that becomes marked by stable PSD-95 assemblies. Note that a neurite positive for SynCAM 1-Cherry is adjacent to the contact site. (B) The graph depicts the progressive increase in PSD95-GFP fluorescence in the contact region of interest (ROI) marked by green boxes in the bottom row of A. Contact between the SynCAM 1-expressing growth cone and PSD-95 positive dendrite occurred at  $t_0$ . The trace shows a fit of the data by a polynomial of the order 3;  $R = 8.0$ .

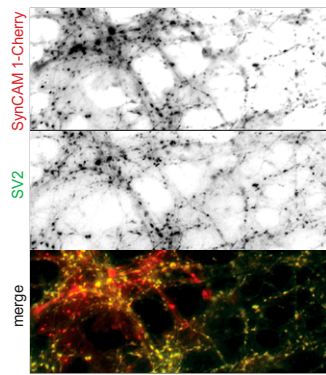


**Fig. 58.** Exogenous SynCAM 1 localizes to mature synapses. Exogenously expressed SynCAM 1 localizes to synaptic sites in mature neurons. SynCAM 1-Cherry (red, *Upper*) was expressed in rat hippocampal neurons, and immunostaining for the presynaptic marker SV2 (green, *Center*) was performed at 25 d.i.v. SynCAM 1-Cherry appears punctate and colocalizes with the synaptic marker SV2 as shown in the merged *Lower* panel.

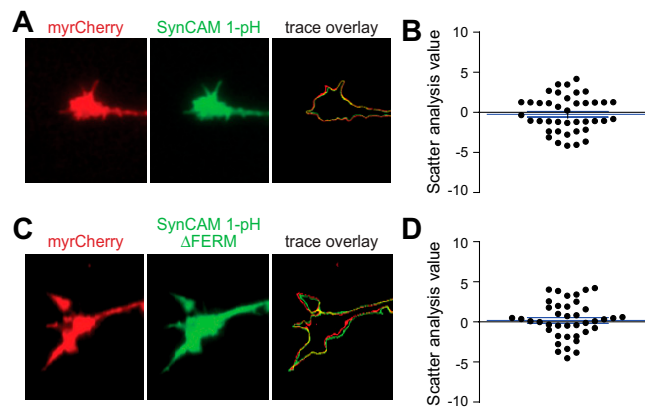


**Fig. 59.** Applicability of SynCAM constructs for Sholl analyses. (A) SynCAM 1-pHluorin traces the complete outline of growth cones. Dissociated rat hippocampal neurons coexpressing the plasma membrane marker myr-Cherry (red, *Left*) and SynCAM 1-pHluorin (green, *Center*) were cultured and imaged live at 5 d.i.v. The *Right* panel shows the overlaid perimeters and demonstrates that they replicate each other. Images were acquired under nonlinear conditions to detect the full fluorescence signal throughout growth cones. (B) Sholl scatter values calculated from traced growth cones coexpressing myrCherry and SynCAM 1-pHluorin. After separate Sholl analysis of images in A, traces determined for myr-Cherry and SynCAM 1-pHluorin yield indistinguishable scatter analysis values for each growth cone [ $\chi^2$  test, Fisher's exact test,  $H(0)$  = difference on samples,  $P$  = not significant, rejected  $H(0)$  hypothesis;  $n$  = 500 images]. (C and D) The comparative analysis of myr-Cherry and SynCAM 1-pHluorin  $\Delta$ FERM distribution was performed as described in A and B. This  $\Delta$ FERM deletion construct traces the complete outline of growth cones ( $P$  = not significant;  $n$  = 500 images).

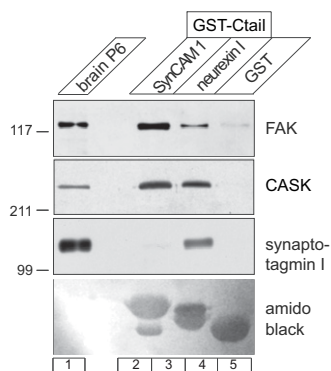
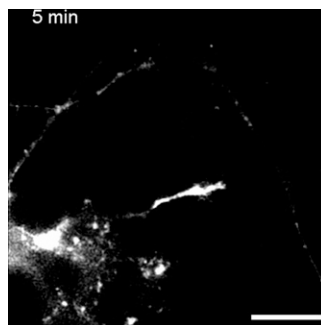


**Fig. 510.** Preferential binding of FAK to SynCAM 1. Rat forebrain proteins were bound to GST fusions of the cytosolic sequence of SynCAM 1 or neurexin I, and fractions were analyzed by immunoblotting for the indicated proteins. Synaptotagmin I binds to neurexin (14), but is not retained on SynCAM 1. Immobilization of equal amounts of GST fusion proteins was controlled by amido black staining of the immunoblots.

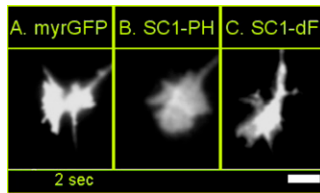
**Table S1. Oligonucleotides used in this study**

Oligo name	Sequence	Template
TB123	CTCGAGCTAGCGGTATGGTGAGCAAGGGCGAG	pHluorin, Cherry
TB124	CACTGGCTAGCTCCCTTGTACAGCTCGTCCATGC	pHluorin, Cherry
TB127	CATCACAGATTCTCGAGCTAGCGAAGAGGGGACCATTGGG	Mouse SynCAM 1
TB139	GGGAAGCTTCTAGATGAAGTACTTTTCTT	Mouse SynCAM 1
TB145	TCTGGGCCGCTATTTTGCC	Mouse SynCAM 1
TB148	CTCGAGCTAGCACCATGGGGAGTAGCAAG	Myristoylation sequence
TB149	GCACTGCTAGCCTCGAGCGGTGGATCCCGGG	Myristoylation sequence
MS027	TCCCCTCTTCACTGCTCGGCTAGCTGTGATGATGGTAAG	Mouse SynCAM 1
MS029	ATTCAGTAGTACCATGGCGAGTGTGTGCTG	Mouse SynCAM 1
MS047	GACCATGGGGAGTAGCAAGAGCAAG	Myristoylation sequence
MS048	GCTTTACTTGTACAGCTCGTCCATG	GFP
MS052	CGCTCGAGCTTTACTTGTACAGCTCGTCCATG	pHluorin, Cherry
MS061	TCAGTGTGGCCGTGTCTGCCCTAGCATTTTC	Mouse FRNK
MS063	CCGCTAGCTCAGTGTGGCCGTGTCTGCCCTAGC	Mouse FAK
MS064	AAGCTAGCGACACCATGGACTGTCTCTGTATAG	Rat PSD-95
MS065	TTGCTAGCTTACTTGTACAGCTCGTCC	Rat PSD-95
MS072	GAGGCTAGCGGTATGAGTAAAGGAGAAGAAC	pHluorin
MS073	TTATTTGTATAGTTCATCCATGCC	pHluorin
LS001	CTAAGTCGACCCGGCAAATAGCGGCCCAGAATGAT GAGCAAGC	Mouse SynCAM 1
LS002	GGGTCGACTCATGAAGCCAAAGGAGCCGATGACGCA GCAGACGC	Mouse SynCAM 1
DA001	GCGGGTACCATGGGCGCTATTTTGCCAGA	Mouse SynCAM 1
DA002	GCGGCGGCCGCTAGATGAAGTACTTTTC	Mouse SynCAM 1
DA003	GCGGCGGCCGCTAGATGAAGTACTTTTCTT	Mouse SynCAM 1



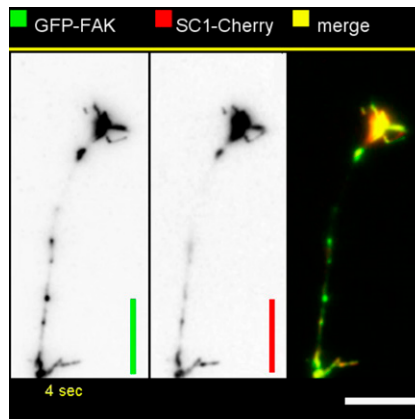
**Movie S1.** SynCAM 1 accumulates and is retained at axo-dendritic contact sites. Dissociated rat hippocampal neurons were transfected with SynCAM 1–pHluorin, and images were acquired at 5 d.i.v. by live microscopy on an Olympus Ix81 microscope in an epifluorescence-like mode with illumination of the complete growth cone volume. The movie shows the images for the observation period (acquisition at 1 frame every 5 min, total acquisition period 240 min; movie rate 2 frames/s). The panels in Fig. 2A were selected from this movie, and the legend of this figure provides additional information. Movie S1, available for download, was compressed by reducing the original quality. (Scale bar: 20  $\mu$ m.)

[Movie S1](#)



**Movie S2.** SynCAM 1 restricts the complexity of growth cones. Exogenous SynCAM 1 reduces apparent growth cone complexity in dependence on its FERM domain interactions. Dissociated rat hippocampal neurons expressing the plasma membrane marker myristoylated GFP (myr-GFP) as negative control (A), SynCAM 1-pHluorin (B), or SynCAM 1-pHluorin  $\Delta$ FERM (C) were imaged live at 5 d.i.v. (acquisition 1 frame every 2 s, total acquisition period 1000 s; movie rate 15 frames/s). The frames shown in Fig. 3 A–C were selected from these recordings, and the legend of this figure provides additional information. Movie S2, available for download, was compressed by reducing the original quality.

[Movie S2](#)



**Movie S3.** The SynCAM 1-FAK complex dynamically enters growth cones and their exploring filopodia. Dissociated rat hippocampal neurons were co-transfected with GFP-FAK (green, *Left*) and SynCAM 1-Cherry (red, *Center*; merge, *Right*) and analyzed at 5 d.i.v. by live two-channel imaging using TIRF microscopy on an Olympus Ix81 microscope (acquisition 1 frame every 4 s, total acquisition period 432 s; movie rate 4 frames/s). GFP-FAK and SynCAM 1-Cherry colocalize within growth cones and dynamically enter exploring filopodia. The frames shown in Fig. 4E were selected from this movie, and the legend of this figure provides additional information. Movie S3, available for download, was compressed by reducing the original quality. (Scale bar: 20  $\mu$ m.)

[Movie S3](#)